Available online at www.sciencedirect.com
SCIENCE DIRECT®
Mechanism and Machine Theory 40 (2005) 977–992
Mechanism and Machine Theory
www.elsevier.com/locate/mechmt

Limit position synthesis and analysis of compliant 4-bar mechanisms with specified energy levels using variable parametric pseudo-rigid-body model

Mohammad H.F. Dado *

Department of Mechanical Engineering, Faculty of Engineering and Technology, University of Jordan, Amman 11942, Jordan

Accepted 15 December 2004
Available online 24 May 2005

Abstract

This paper provides a synthesis and analysis procedure for the limit positions of compliant 4-bar mechanisms. The mechanism compliance is present at the output link which is considered to be fixed to the ground and can experience large non-linear elastic deflection at its pinned end. Under this condition, the mechanism mobility and its limit positions are dependent on the output link compliance. In addition, an elastic potential energy is stored at each limit position with a magnitude depending on the mechanism geometry and output link compliance properties. The developed procedure provides means of determining the complete mechanism geometry for (1) specified limit positions, or (2) specified energy level at each limit position. On the analysis side, the procedure provides the limit positions and energy levels for specified mechanism geometry. The compliant output link is modeled using the variable parametric pseudo-rigid-body model. In this model, the pseudo-rigid-body parameters vary for different loading conditions, thus, providing a more accurate model than that with fixed parameters. The procedure is presented in form of charts with minimum computational effort by the user. Illustrative examples are presented to prove the utility of the developed procedure.

* Tel.: +962 6 535 5000; fax: +962 6 535 5588.
E-mail address: dado@ju.edu.jo

0094-114X/$ - see front matter © 2005 Elsevier Ltd. All rights reserved.
doi:10.1016/j.mechmachtheory.2004.12.013

Keywords: Compliant mechanisms; Limit positions; Pseudo-rigid-body model

1. Introduction

The motion in compliant mechanisms is gained by the large deflection of its flexible members instead of the rigid-body motion provided by its kinematic pairs. This characteristic of compliant mechanisms gives it an important advantage over conventional mechanisms as it reduces manufacturing and operating costs and eliminates noise and wear of regular kinematic pairs [1]. In addition, the compliance provides additional variables for design improvement. Many researchers developed models and procedure for the synthesis and analysis of compliant linkages. A synthesis procedure for a planar four-bar linkage with flexible coupler link was developed by Burns and Crossley [2]. Midha et al. [3] used a numerical technique to analyze large deflection of elastic links and applied it in the design of compliant mechanisms. Howell and Midha [4] developed a pseudo-rigid-body model for large deflection beams. They found the optimum fixed parameters for the model so that the end point deflection of the beam is approximated with minimum error. Dado [5] developed a similar model but with variable parameters so that the error is minimized for a wide range of motion of the end point. He applied the developed model in an analysis procedure for compliant mechanisms. Howell and Midha [6] applied the loop closure equations for the analysis and synthesis of compliant mechanisms. They performed dimensional synthesis for specific motion programming requirements.

Determining the limit positions of compliant 4-bar mechanisms is of practical value. A non-linear torsional spring behavior is produced by driving a compliant 4-bar mechanism through its limit positions. The driving torque at each limit position is zero and varies non-linearly in between. In addition, three equilibrium positions may exist. Two are for the two limit positions and they are unstable while the third is stable and corresponds to the un-deflected position of the compliant link. Mechanisms with these drive/motion characteristics could be used in electrical switches and in machines with non-linear spring action requirements. Midha, Howell and Norton [7] presented a method for determining the limit positions of compliant 4-bar mechanisms using the pseudo-rigid-body model concept. They introduced a method for determining the limit positions of different compliant 4-bar mechanism configurations using the pseudo-rigid-body model with fixed parameters. In the method presented, the mechanism is converted to its, approximately, equivalent rigid-body model and the well established rigid-body mechanism procedures are applied on the equivalent model. In this paper, a synthesis and analysis procedure for the limit positions of compliant 4-bar mechanisms is presented. The output link is considered to be fixed to the ground and can experience large non-linear elastic deflection at its pinned end. The mechanism mobility, its limit positions and the elastic potential energies stored at these limit positions are function of the output link compliance. The compliant output link is modeled using the variable parametric pseudo-rigid-body model developed by Dado [5]. The parameters of the pseudo-rigid-body are dependent on the load magnitude and direction at the free end. This improved model provides an accurate representation of the compliant link behavior and covers a wide range of free end deflection. The procedures presented in the following sections provide synthesis as well as analysis tool for the limit positions and the associated stored elastic strain energies for the compliant 4-bar mechanism.

2. The variable parametric pseudo-rigid-body model

The variable parametric pseudo-rigid-body model developed by Dado [5] is based in principle on the fixed parameters model developed by Howell and Midha [4]. Figs. 1 and 2 illustrate the model and its parameters. Fig. 1(a) shows a flexible cantilever beam and its corresponding deflected geometry. The beam has a length l and it is subjected to the end load P acting at angle ϕ with respect to the un-deflected beam axis. Fig. 1(b) shows the corresponding pseudo-rigid-body model of the beam in which the beam is modeled by two rigid segments joined by a pivot. As represented by the figure, the moving segment length is γl and the fixed segment length is $(1-\gamma)l$. In addition, the torsional spring has a stiffness K and it is located at the pivot between the two segments. The parameter γ is called the characteristic length ratio and the angle Θ shown in the figure is called the pseudo-rigid-body angle and the pivot joining the two segments is called the characteristic pivot. According to [4], the fixed optimum value of $\gamma = 0.85$ and that for $K = 2.56\frac{EI}{l}$, where E is the modulus of elasticity of the beam material and I is the area moment of inertia of its cross-section. Using the variable parametric model, the model parameters are related as follows:

$$K = f_k(\gamma, \Theta)\frac{EI}{l} \tag{1}$$

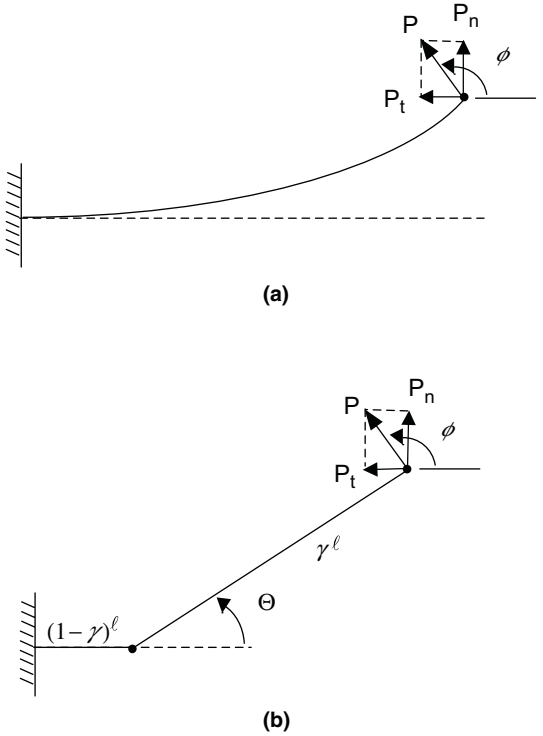

Fig. 1. (a) A compliant link experiencing large deflection due to end load, (b) its pseudo-rigid-body model.

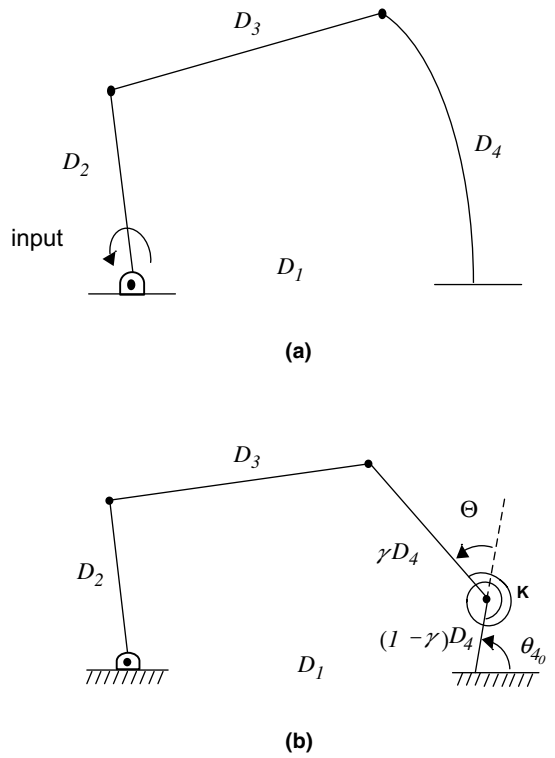

Fig. 2. (a) A four-bar mechanism with a compliant output link, (b) its pseudo-rigid-body model.

and

$$P_n = f_p(\gamma, \Theta)\frac{EI}{l^2} \tag{2}$$

where P_n is the end load component normal to the un-deflected beam axis. Eqs. (1) and (2) express the model's stiffness K and load P_n in terms of the model's kinematics parameters γ and Θ. These two kinematic parameters are accounted for by the loop closure equations and the static equilibrium equations of the mechanism using the expressions for k and P given by Eqs. (1) and (2). The expressions for the functions in Eqs. (1) and (2) are obtained through regression analysis and are given by Dado [5]. These expressions are repeated here for convenience as follows:

$$f_k(\gamma, \Theta) = \sum_{i=1}^{4}\sum_{j=1}^{4} a_{ij}^k \gamma^{m_i^k}\Theta^{l_j^k} \tag{3}$$

$$f_p(\gamma, \Theta) = \sum_{i=1}^{4}\sum_{j=1}^{4} a_{ij}^p \gamma^{m_i^p}\Theta^{l_j^p} \tag{4}$$

The values of the coefficients a_{ij}^k and a_{ij}^p for the indicated powers of γ *and* Θ are given in Ref. [5].

3. The limit positions model of the compliant mechanism

The compliant four-bar mechanism under consideration is shown in Fig. 2(a). It is a regular four-bar mechanism except that the output or follower link is not pinned to the ground but instead it is fixed. Considering the input and coupler links as rigid links, gross kinematic motion could take place only if the output link is highly flexible or compliant. The driving torque at the input link must resist the nonlinear spring action due to the motion of the end-point of the output link. The compliant mechanism is modeled as shown in Fig. 2(b), where the output compliant link is replaced by its equivalent pseudo-rigid-body model. The loop closure equation for this model is

$$D_2\vec{U}_{\theta_2} + D_3\vec{U}_{\theta_3} = D_1\vec{U}_0 + (1-\gamma)D_4\vec{U}_{\theta_{40}} + \gamma D_4\vec{U}_{\theta_4} \tag{5}$$

where $\vec{U}_\beta$ is a unit vector in the Cartesian coordinate system with an angular orientation β and defined as $\vec{U}_\beta = \cos\beta\vec{i} + \sin\beta\vec{j}$. The fixed link length could be used as a scaling factor for the whole mechanism so that it is considered to have a value of unity and all other lengths are multiples of its actual length. Note that the pseudo-rigid-body angle Θ is given as

$$\Theta = \theta_4 - \theta_{40} \tag{6}$$

The modeled mechanism at its two limit positions is shown in Fig. 3(a). The loop closure equation at the two limit positions with the scaled link lengths $d_j = D_j/D_1$ (*for* $j = 1,2,3,4$) is written as

$$\gamma d_4\vec{U}_{\theta_4} = d_{23}\vec{U}_{\theta_2^*} - \vec{U}_0 - (1-\gamma)d_4\vec{U}_{\theta_{40}} \tag{7}$$

where $d_{23} = d_{23,1} = d_2 + d_3$ for the extended position, position 1, at which $\theta_2^* = \theta_{21}$ and $d_{23} = d_{23,2} = d_3 - d_2$ for contracted position, position 2, at which $\theta_2^* = \theta_{22} - \pi$. Eq. (7) is to be combined with the moment equilibrium equation at the characteristic pivot to solve for γ, d_{23}, and θ_4 for specified values of θ_{40}, d_4, and θ_2^*. The results are to be manipulated in a manner that serves the goals stated earlier for this study. To eliminate θ_4, dot product each side of Eq. (7) by itself to obtain

$$\begin{aligned}\gamma^2 d_4^2 = {} & -2d_{23}\cos\theta_2^* + d_{23}^2 - 2d_{23}(1-\gamma)d_4\cos(\theta_2^* - \theta_{40}) + 1 \\ & + 2(1-\gamma)d_4\cos\theta_{40} + (1-\gamma)^2 d_4^2\end{aligned} \tag{8}$$

Rearrange Eq. (8) as

$$d_{23}^2 - 2ad_{23} + b = 0 \tag{9}$$

where

$$a = \cos\theta_2^* + (1-\gamma)d_4\cos(\theta_2^* - \theta_{40})$$

$$b = 1 + 2(1-\gamma)d_4\cos\theta_{40} + (1-\gamma)^2 d_4^2 - \gamma^2 d_4^2$$

From Eq. (9), d_{23} is determined by

$$d_{23} = a \pm \sqrt{a^2 - b} \tag{10}$$

The sign before the radical is chosen to be positive for the results presented latter. The choice of the negative sign is equivalent to an equal but negative value of d_{23} resulting from the first choice but with an angular direction of either $(\theta_2^* + \pi)$ or $(\pi - \theta_2^*)$ as could be observed form

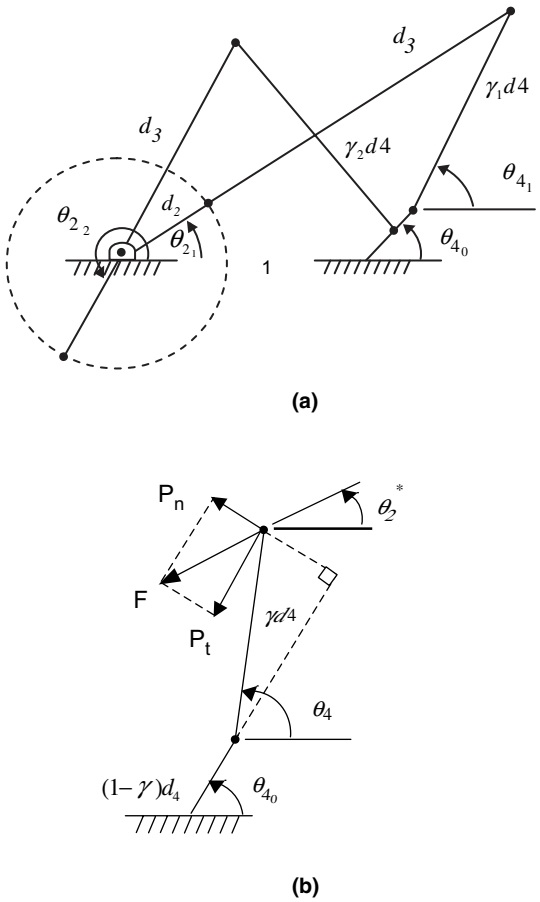

Fig. 3. (a) The pseudo-rigid-body model of the compliant four-bar at it two limit positions, (b) the compliant link model.

the expression of the intermediate variable a and Eq. (10). Therefore, one choice leads to the other with the observation of proper directions. The angle θ_4 is determined in terms of the parameter γ using the vector equation given by Eq. (7) as

$$\theta_4 = \tan^{-1}\left(\frac{d_{23}\sin\theta_2^* - (1-\gamma)d_4\sin\theta_{40}}{d_{23}\cos\theta_2^* - 1 - (1-\gamma)d_4\cos\theta_{40}}\right) \tag{11}$$

The characteristic length parameter γ is solved for by writing a moment balance equation at the characteristic pivot of the pseudo-rigid-body model of the output compliant link. Considering Fig. 3(b), the axial force F of the coupler link is given as

$$F = \frac{P_n}{\sin(\theta_{40} - \theta_2^*)} \tag{12}$$

The moment produced by the force F at the pivot is

$$M_F = \gamma d_4 F \sin(\theta_4 - \theta_2^*) \tag{13}$$

This moment is equal to the characteristic spring resistance at the pivot. Therefore, the following equilibrium equation could be written

$$M_F = (\theta_4 - \theta_{40})K \tag{14}$$

Substitute for P_n and K their equivalents given by Eqs. (1) and (2), use Eqs. (12) and (13), and set $l = d_4$ to obtain the following relation

$$(\theta_4 - \theta_{40}) f_K(\gamma, \theta_4 - \theta_{40}) \sin(\theta_{40} - \theta_2^*) - \gamma \sin(\theta_4 - \theta_2^*) P_n(\gamma, \theta_4 - \theta_{40}) = 0 \tag{15}$$

For given values of θ_{40}, θ_2^*, *and* d_4 and by substituting for θ_4 using Eq. (11), the only remaining unknown in Eq. (15) is γ. An iterative procedure using Newton–Raphson technique with numerical differentiation is applied on Eq. (15) to solve for γ. A very good initial guess for γ is its value in the fixed parameter pseudo-rigid-body model given by [4] as 0.85. Once γ is found within reasonable accuracy, the values of d_{23} *and* θ_4 are computed using Eqs. (10) and (11), respectively.

4. Stored strain energy

Strain energy is stored when the compliant link is deflected from its un-loaded position. The stored energy is directly related to the pseudo-rigid-body angle Θ and the characteristic length ratio γ. By direct integration of Eq. (1) with respect to Θ for given values of γ, the stored energy, E_s, is determined as

$$E_s = \frac{EI}{D_4} E_f \tag{16}$$

where E is the modulus of elasticity of the compliant link, I is its cross-section area moment of inertia and D_4 is the actual length of link 4. E_f is a dimensionless strain energy factor obtained by integrating the function $f_k(\gamma, \Theta)$ of Eq. (3) for a given value of γ. Fig. 4 plots the values of E_f for a range of Θ and selected values of γ. Note that the energy factor values for Θ is the same for $\Theta \leqslant 0$ since $f_k(\gamma, \Theta)$ is an even function on Θ.

5. Results

Eqs. (10), (11) and (15) are solved in a manner that charts could be generated for syntheses and analysis purposes. Several values of both θ_{40} and d_4 are chosen. For all possible combinations of these chosen values and for a full 0 *to* 2π range of θ_2^*, the values of d_{23} *and* $\Theta = \theta_4 - \theta_{40}$ are tabulated. Several charts are generated so that each chart belongs to one chosen value of θ_{40}. In each chart several curves are plotted corresponding to the chosen values of d_4. The horizontal axis represents the values of θ_2^* and the two vertical axes give the values of d_{23} *and* Θ so that for each value of d_4 two curves exist, one for θ_2^* vs. d_{23} and the other for θ_2^* vs. Θ. These charts are shown in Figs. 5–9. Note that for the chosen values of θ_{40}, 30°, 60°, 90°, 120°, *and* 150°, the same results apply for

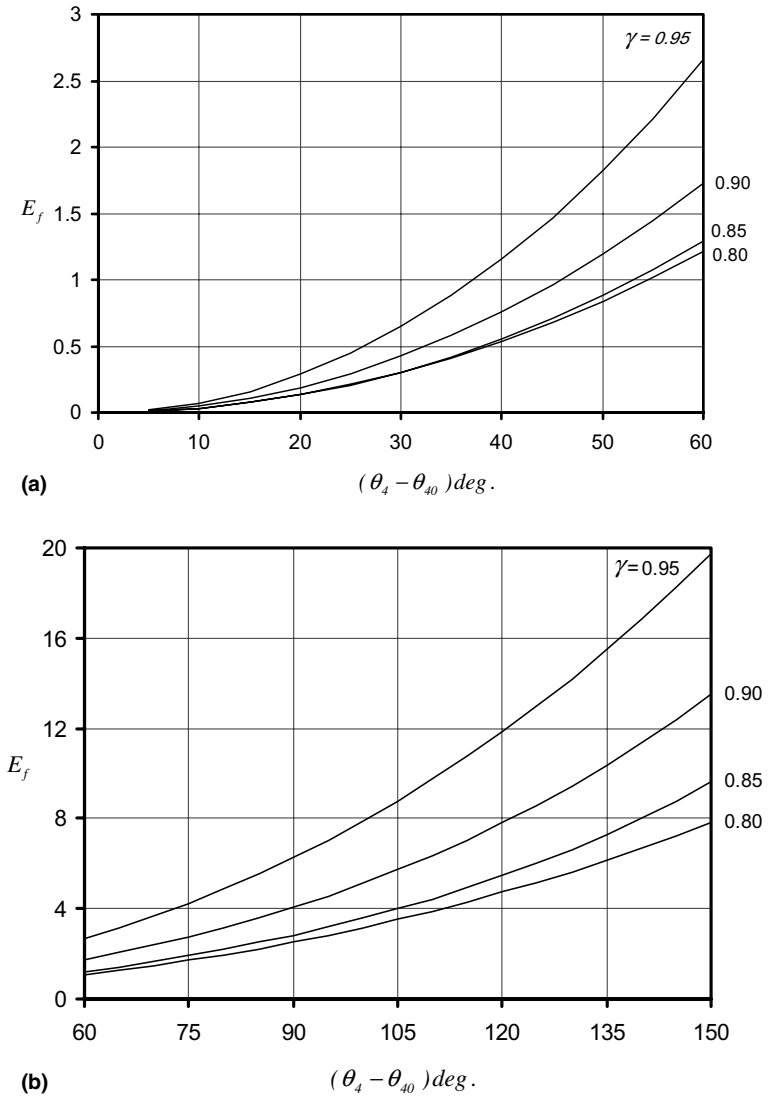

Fig. 4. The stored energy in the compliant link for different characteristic length ratio γ verses $\Theta = \theta_4 - \theta_{40}$.

their mirror image values, $-30°$, $-60°$, $-90°$, $-120°$, *and* $-150°$, about the fixed link axis. Of course, the same sign conversion must be done for θ_2^*.

As observed from these charts, not the full range of θ_2^* is present. This is due to the fact that the mechanism does not exist at particular combinations of θ_{40}, θ_2^*, *and* d_4. These combinations occur if the term under the radical in Eq. (10) is less than zero. Another reason for the missing data is that the pseudo-rigid-body angle Θ should be in the range $-145° \leqslant \Theta \leqslant 145°$ and the characteristic length ratio γ should be in the range $0.75 \leqslant \gamma \leqslant 0.95$ for acceptable accuracy of the model, Dado [5]. These cases are omitted from the results after attempting the solution of Eq. (15) using the full range of acceptable values for the initial guess of the characteristic length ratio, γ.

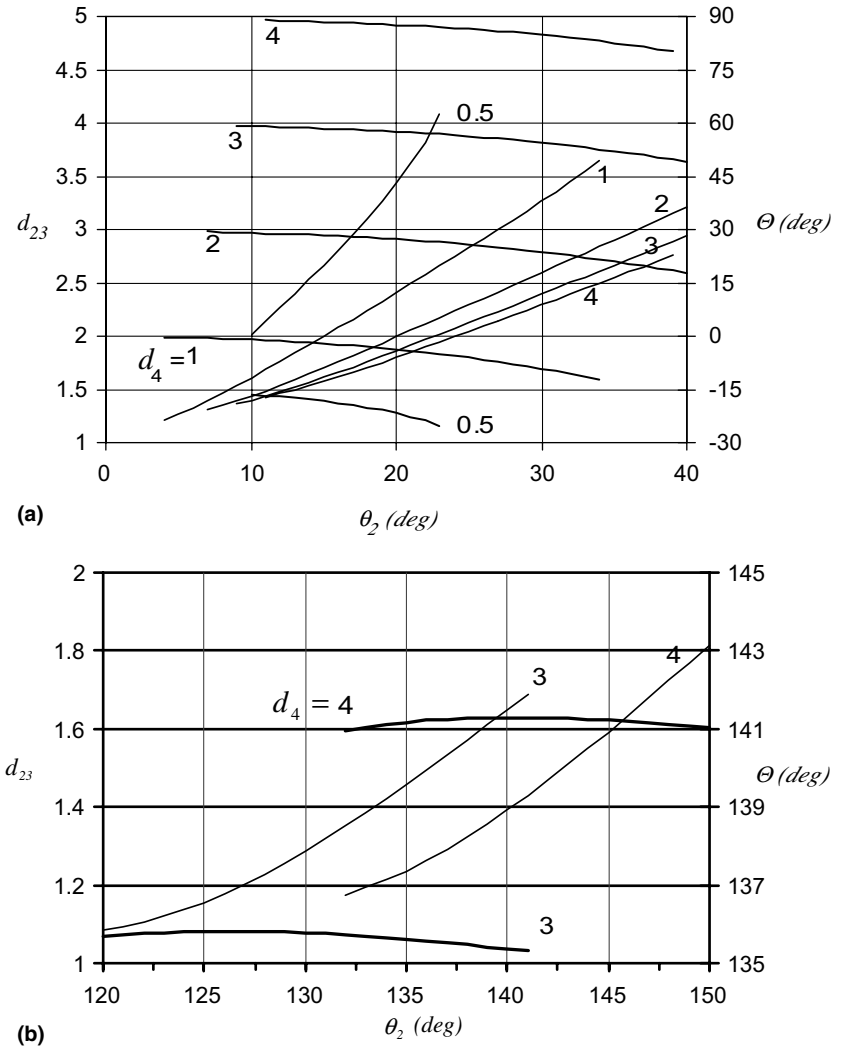

Fig. 5. The mechanism parameters for $\theta_{40} = 30°$. ——— d_{23} and —— $\Theta = \theta_4 - \theta_{40}$.

6. The syntheses and analysis procedures

The solution charts are suitable for two modes of syntheses: (1) finding the mechanism dimensions for specified limit positions, (2) finding the mechanism dimensions for specified energy storage at each limit position. For the first mode, one may specify the compliant link orientation at its fixed end represented by θ_{40}. This step identifies which chart to use. As a second step, one may specify the required angles at which the limit positions must occur. Note that for the extended position, position 1, $\theta_2^* = \theta_{21}$ and for the retracted position, position 2, $\theta_2^* = \theta_{22} - \pi$. This leads to several values for d_4 and for each value thereof two values for d_{23} and Θ corresponding to the two limit positions. After selecting the desired combination, the input and coupler link lengths are obtained as

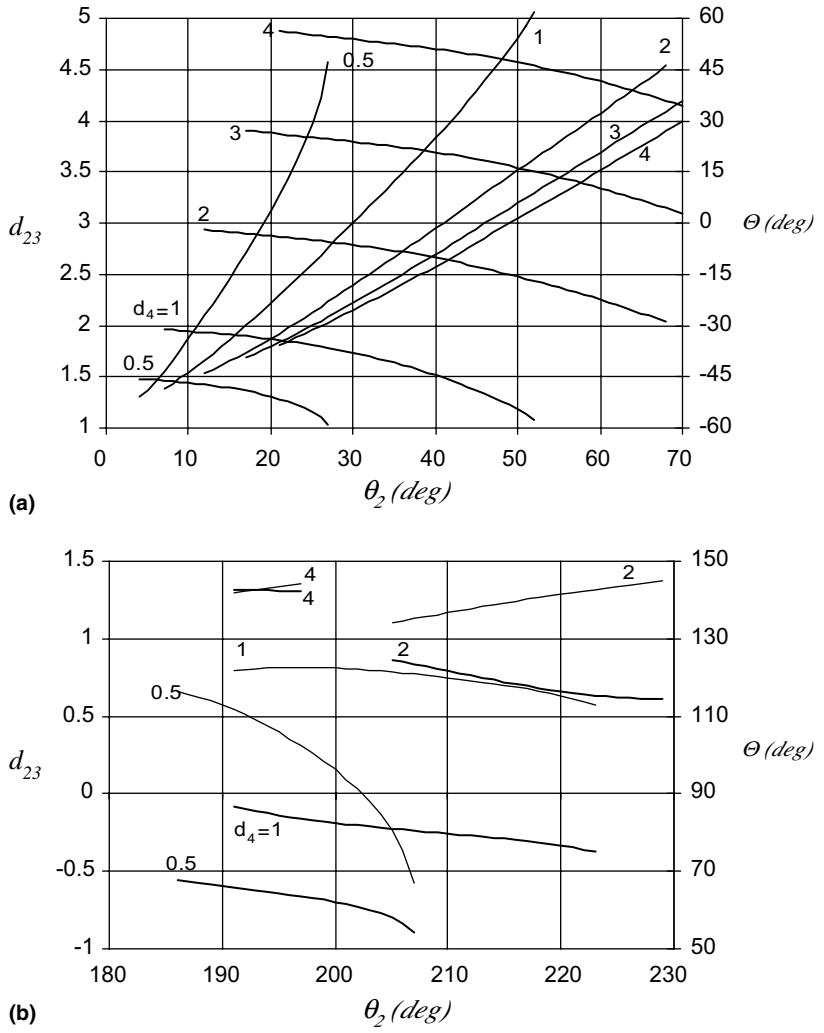

Fig. 6. The mechanism parameters for $\theta_{40} = 60°$. ——— d_{23} and —— $\Theta = \theta_4 - \theta_{40}$.

$$d_2 = (d_{23,1} - d_{23,2})/2 \tag{17}$$

$$d_3 = (d_{23,1} + d_{23,2})/2 \tag{18}$$

For the second mode of syntheses, the stored energy must be first defined in terms of the mechanism kinematic parameters. From Fig. 4 and for a specific value of E_f, the angle Θ is obtained for a trial value of γ. With this value of Θ, a selected chart corresponding to a specific θ_{40} and a suitable value for d_4, the limit position angle θ_2^* and the length d_{23} are obtained. If these parameters could not be realized from the selected chart, a different chart must be tried. After the proper selections are made, the trial value of γ must be checked. The updated value of γ corresponding to the selections is defined using Eq. (7) as

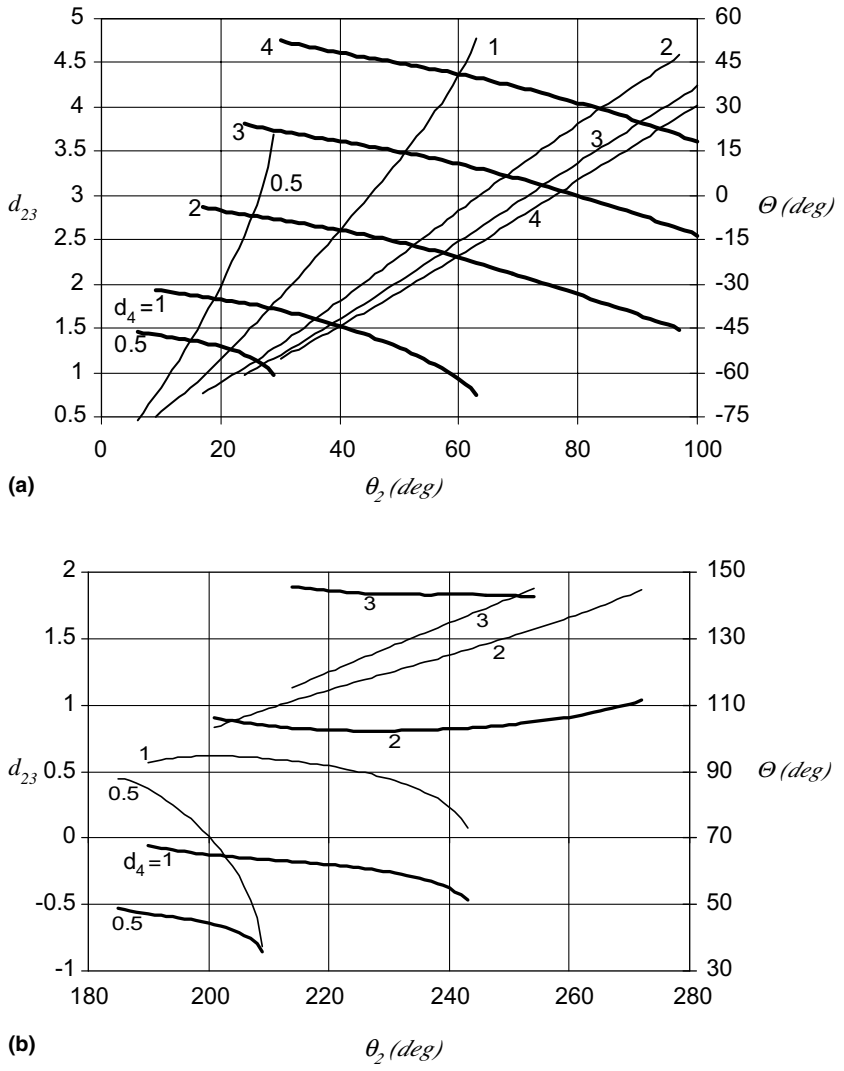

Fig. 7. The mechanism parameters for $\theta_{40} = 90°$. ——— d_{23} and —— $\Theta = \theta_4 - \theta_{40}$.

$$\gamma = \frac{d_{23}\cos\theta_2^* - 1 - d_4\cos\theta_{40}}{d_4(\cos\theta_4 - \cos\theta_{40})} \tag{19}$$

If the updated value of γ is not within acceptable accuracy of the trial value, the process is repeated using the updated value of γ. This iterative process continues until the desired accuracy is reached. A good first trial for γ is its fixed parameters pseudo-rigid-body model value of 0.85 as given in [4].

The analysis procedure is straight forward. For given values of θ_{40} *and* d_4 a chart and a curve on this chart are specified. For the extended position, the value $d_{23,1} = d_2 + d_3$ is specified and the corresponding limit position $\theta_{21} = \theta_2^*$ is determined. Similarly, for the retracted position, the value $d_{23,2} = d_3 - d_2$ is specified and the corresponding limit position $\theta_{22} = \theta_2^* - \pi$ is determined.

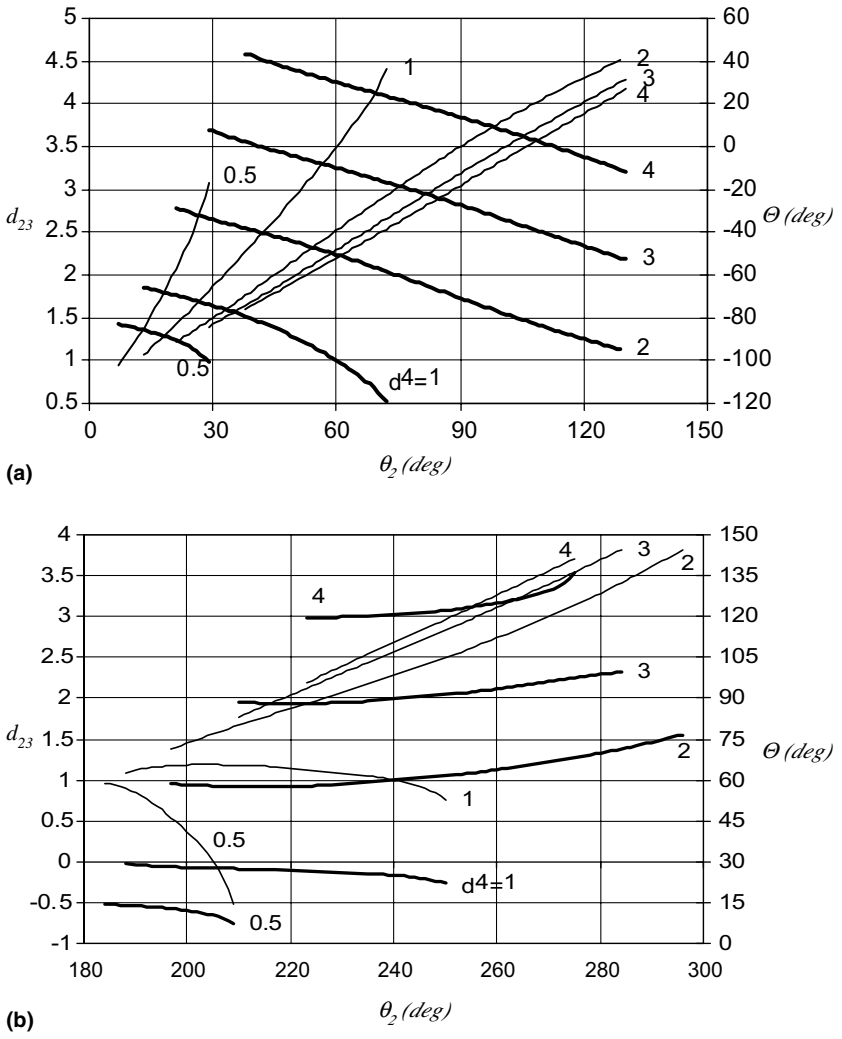

Fig. 8. The mechanism parameters for $\theta_{40} = 120°$. ——— d_{23} and —— $\Theta = \theta_4 - \theta_{40}$.

7. Illustrative examples

Three illustrative examples are presented, two examples for the two types of syntheses procedures and one example for the analysis procedure with a comparison with the fixed parameter model of [7].

7.1. Example 1: Given the two limit positions.

Given: $\theta_{21} = 30°$ *and* $\theta_{22} = 270°$
Find: The mechanism dimensions and the stored energy at each position.

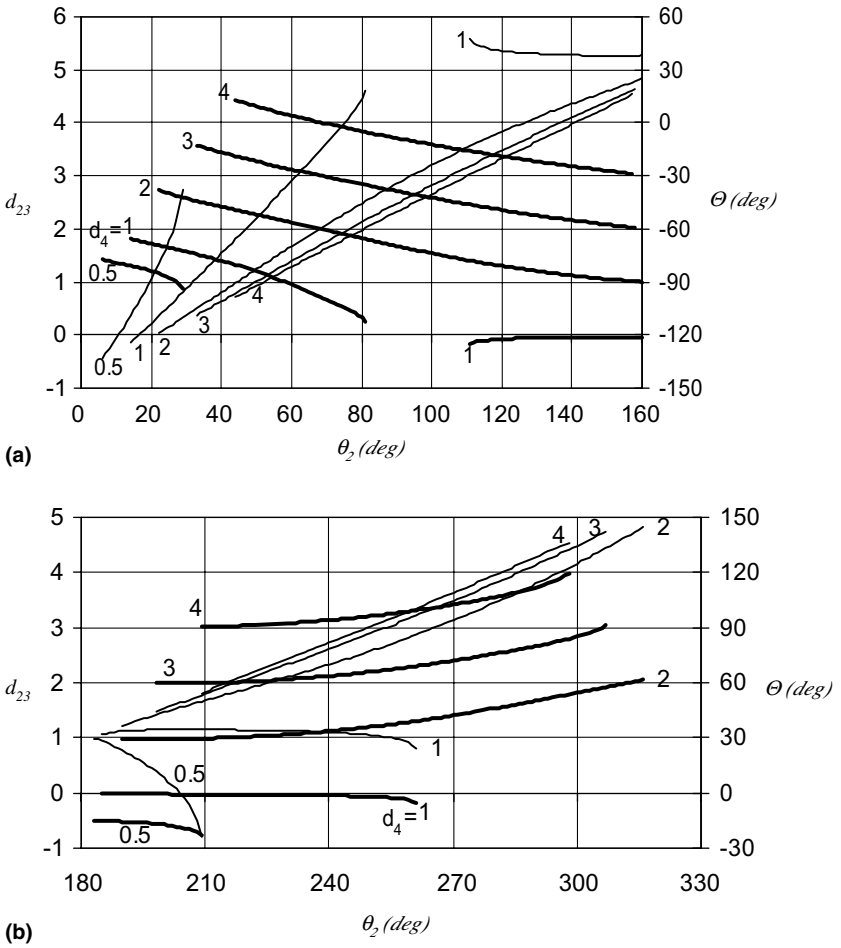

Fig. 9. The mechanism parameters for $\theta_{40} = 150°$. ——— d_{23} and —— $\Theta = \theta_4 - \theta_{40}$.

Solution: 1.

1. Re-define the limit positions as $\theta_{21}^* = \theta_{21} = 30°$ *and* $\theta_{22}^* = \theta_{22} - 180° = 90°$.
2. Chose the chart of $\theta_{40} = 120°$ and the curve $d_4 = 2$. These choices are made since they include the two limit positions in (1).
3. Read the values of $d_{23,1}$ *and* $d_{23,2}$ from the chart as 2.65 and 1.57, respectively.
4. Determine the input and coupler link lengths using Eqs. (17) and (18) as 0.54 and 2.11, respectively.
5. Read the pseudo-rigid-body angles form the chart as $\Theta_1 = -80°$ *and* $\Theta_2 = 0°$.
6. Determine the stored energy factor E_f for the extended position by finding γ_1 using Eq. (19) as 0.91 and reading its value from Fig. 4 as 4.5. There is no stored energy at the retracted position since $\Theta_2 = 0$.

Fig. 10(a) shows the synthesized mechanism at its two limit positions.

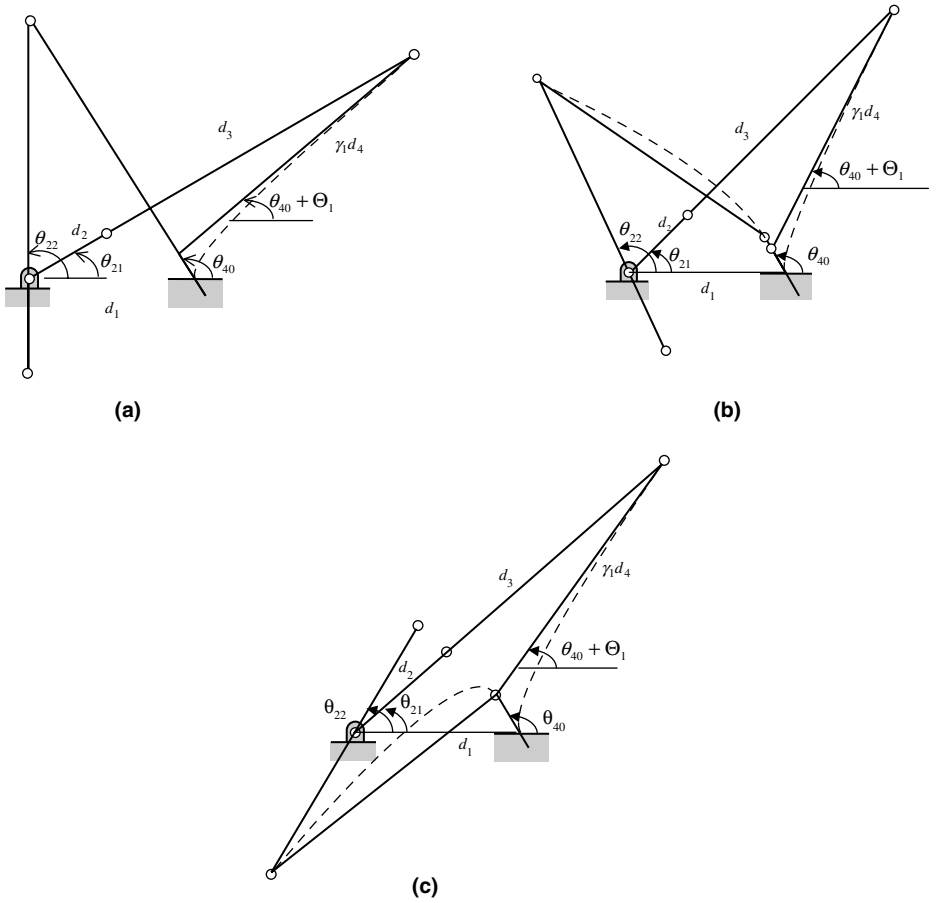

Fig. 10. The example mechanisms at their limit positions; (a) example 1, (b) example 2 and (c) example 3.

7.2. Example 2: Given the stored energy factors at the two limit positions.

Given: $E_{f1} = 1.0$ *and* $E_{f2} = 3.0$
Find: The mechanism dimensions and the corresponding limit positions.
Solution:

1. For the first position, assume the trial value of γ_1 as 0.85 so that from Fig. 4, $\Theta_1 = 25°$.
2. For the second position, assume the trial value of γ_2 as 0.85 so that from Fig. 4, $\Theta_2 = -80°$.
3. Chose the chart of $\theta_{40} = 120°$ and the curve $d_4 = 2$. These choices are made since they include Θ_1 *and* Θ_2 found in (1) and (2).
4. Read the values of $d_{23,1}$ *and* $d_{23,2}$ from the chart as 1.35 and 2.65, respectively.
5. Read the two limit position angles θ^*_{21} *and* θ^*_{22} as 115° *and* 30°, respectively.
6. Compute the new values of the characteristic length ratios γ_1 *and* γ_2 using Eq. (19) as 0.86 and 0.9, respectively. The value for γ_1 is acceptable compared to the initial trial of 0.85 but the value for γ_2 needs more iterations.

7. The value of Θ_2 corresponding to $\gamma_2 = 0.9$ is $-55°$ leading to $d_{23,2} = 2.4$ *and* $\theta^*_{22} = 45°$. The new value of γ_2 is 0.91 which is close enough to the previous trial value of 0.9.
8. The resulting mechanism dimensions are: $d_2 = 0.525$, $d_3 = 1.875$, *and* $d_4 = 2.0$. E_{f1} occurs at the retracted position at $\theta_{21} = 115 + 180 = 295°$ and E_{f2} occurs at the extended position at $\theta_{22} = 45°$.

Fig. 10(b) shows the synthesized mechanism at its two limit positions.

7.3. Example 3: Given the mechanism dimensions

Given: $d_2 = 0.75$, $d_3 = 1.75$, $d_4 = 2$, *and* $\theta_{40} = 120°$.
Find: The two limit positions and the stored energy at each position (a) using the variable parameter model and (b) using the fixed parameter model of Ref. [7].
Solution: (a)

1. Compute $d_{23,1}$ *and* $d_{23,2}$ as 2.5 and 1.0, respectively.
2. Chose the chart of $\theta_{40} = 120°$ and the curve $d_4 = 2$.
3. Read the values of θ^*_{21} *and* θ^*_{22} as 42° *and* 240°, respectively. The extended limit position is at $\theta_{21} = 42°$ and the retracted position is at $\theta_{22} = 240 - 180 = 60°$.
4. Read the pseudo-rigid-body angles form the chart as $\Theta_1 = -65°$ *and* $\Theta_2 = 98°$.
5. Determine the stored energy factors E_{f1} and E_{f2} for the two limit position by finding γ_1 *and* γ_2 using Eq. (19) as 0.86 and 0.87. The stored energy factors are read from Fig. 4 as $E_{f1} = 2.5$ *and* $E_{f2} = 4.0$.

Fig. 10(c) shows the analyzed mechanism at its two limit positions.
Solution: (b)

1. Solving Eq. (7) for θ^*_2 *and* θ_4 at the two limit positions using $\gamma = 0.85$, yields $\theta_{21} = 38°$, $\theta_{22} = 69°$ and $\Theta_1 = -71°$, $\Theta_2 = 105°$.
2. For a constant value of $k = 2.56$, the stored energy at the two limit positions are $E_{f1} = 3.2$ *and* $E_{f2} = 4.7$.

The two solutions of (a) and (b) compares well since the values of γ_1 *and* γ_2 are close to its value of 0.85 in the fixed parameter model. The stored energies values are not as close, though. This behavior is consistent with the conclusions in Ref. [5]. However, if the values of γ_1 *and* γ_2 are not as close, the results are expected to differ much more.

8. Conclusions

Syntheses and analysis procedures for the limit positions of compliant four-bar mechanisms are presented in this paper. These procedures serve as powerful tools in dealing with such mechanisms. The syntheses procedure provides the mechanism dimensions for specified limit positions or specified stored strain energy at each position while the analysis procedure delivers the two limit positions for specified mechanism dimensions. A numerical example for each of these cases is

presented using the charts. The accuracy of the results depends on the accuracy by which the charts are read. For more accurate results, the equations on which the charts are based must be solved for the specific cases of either syntheses or analysis. As an extension for this study, different types of mechanisms and configurations need to be considered.

Acknowledgement

This work was performed during a sabbatical leave at the Department of Mechanical Engineering, The Hashemite University, Zarka – Jordan.

References

[1] N.M. Sevak, C.W. McLarnan, Optimal synthesis of flexible link mechanisms with large static deflections, ASME Paper No. 74-DET-83, 1974.
[2] R.H. Burns, F.R.E. Crossley, Kinetostatic synthesis of flexible link mechanisms, ASME Paper No. 68-Mech-36, 1968.
[3] A. Midha, I. Her, B.A. Salamon, A methodology for compliant mechanism design: Part I—Introduction and large-deflection analysis, in: D.A. Hoeltzel (Ed.), Advances in Design Automation, DE-Vol. 44-2, 18th ASME Design Automation Conference, 1992, pp. 29–38.
[4] L.L. Howell, A. Midha, Parametric deflection approximation for end-loaded, large-deflection beams in compliant mechanisms, Journal of Mechanical Design, Trans. ASME 117 (1) (1995) 156–165.
[5] M.H. Dado, Variable parametric pseudo-rigid-body model for large-deflection beams with end loads, International Journal of Non-linear Mechanics 36 (7) (2001) 1123–1133.
[6] L.L. Howell, A. Midha, A loop-closure theory for the analysis and synthesis of compliant mechanisms, Journal of Mechanical Design, Trans. ASME 116 (4) (1994) 1115–1121.
[7] A. Midha, L.L. Howell, T.W. Norton, Limit positions of compliant mechanisms using the pseudo-rigid-body model concept, Mechanism and Machine Theory 35 (1) (2000) 99–115.